

A New Architecture for Transparent Electrodes: Relieving the Trade-Off Between Electrical Conductivity and Optical Transmittance

Ping Kuang, Joong-Mok Park, Wai Leung, Rakesh C. Mahadevapuram, Kanwar S. Nalwa, Tae-Geun Kim, Sumit Chaudhary,* Kai-Ming Ho,* and Kristen Constant*

Transparent conducting electrodes with the combination of high optical transmission and good electrical conductivity are essential and desirable in solar energy harvesting and electric lighting devices including organic solar cells and light-emitting diodes (LEDs) as well as in their inorganic counterparts. Currently, indium tin oxide (ITO) coated glass is most often used because ITO has relatively high transparency to visible light and low sheet resistance for electrical current conduction. However, ITO is costly due to limited resources, is brittle,^[1] and has poor chemical compatibility with the active organic materials.^[2] These disadvantages have motivated the search for other conducting electrodes with similar or better optical and electrical properties. In recent research efforts, carbon nanotube networks, unpatterned thin metal films, random silver metal nanowire meshes, graphene films, and patterned metal nanowire grids have been evaluated as potential replacements for ITO electrodes.^[3–11] Although these alternative transparent electrode approaches do have the potential to replace ITO, they still suffer from the classic trade-off between the optical transmittance and electrical conductivity. Thicker layers offer higher conductivity, but this comes at the expense of optical transmittance, and vice versa. Here, we report a new architecture for

transparent electrodes, which leads to quasi-elimination of this tradeoff. This architecture consists of high-aspect-ratio metallic ribbons with nanoscale thickness and microscale width, spaced at desired periodicities and held in place by a polymer matrix to provide a flat top surface for fabrication of active layers in solar cells or LEDs. By design, the light path is only obstructed by the nanoscale thickness of the ribbons, thus decoupling the conductivity and transmittance properties from each other. Catrysse and Fan performed theoretical investigations on similar nanopatterned metallic structures, and their simulations indicate that such structures have excellent optical and electrical properties for potential use as transparent conductive electrodes.^[12] Our experimental results show that the novel structure is very promising for such applications.

These structures were fabricated in a multistage process. First, a polyurethane (PU) grating structure with a periodicity of 2.5 μm was fabricated on glass substrate by two-polymer micro-transfer molding (2-P μTM)^[13] (Figure 1a). Metal films, such as gold and silver, were thermally evaporated onto the sample. To ensure higher transparency, two oblique angle depositions were used. The sample was tilted 45° to the normal direction of the source so the PU bar itself would act as shadow mask to block the metal from being deposited on the bottom of the trench. The depositions were done by coating the left sidewall and top of the PU bars and then repeating from the right. Therefore, only the PU surface was coated with metal films (Figure 1b). In order to achieve even higher transmission, the metal on top of the PU bars was removed. We employed argon ion milling, a physical etching technique, to physically remove the metal by ion bombardment. It has been shown that argon ion milling is capable of etching metals such as gold and silver, and it can even be used to remove oxide for nanostructure fabrication.^[14,15] Since the argon milling is directional, when the ion beam direction is parallel to that of PU grating, only the metal on top of the PU grating is removed, leaving the two metallic sidewalls intact (Figure 1c). Furthermore, low angle ion milling (10°) was chosen for controllable metal etching rate and reduction of the PU top surface roughness induced during the milling process (Figure 1d,e). It should be noted that other ion etching methods, including the reactive ion etching (RIE) technique, are also viable for the removal of metal layers,^[16,17] provided the process is directional in order to preserve the metal on the PU sidewalls.

Figure 2a,b show scanning electron microscopy (SEM) images of the PU grating structure on a 200- μm -thick glass substrate at both high and low magnifications. The PU grating

P. Kuang, R. C. Mahadevapuram, Prof. K. Constant
Department of Materials Science and Engineering
Iowa State University
Ames, IA 5001, USA
E-mail: constant@iastate.edu

Prof. K.-M. Ho
Department of Physics and Astronomy
Iowa State University
Ames, IA 50011, USA
E-mail: kmh@iastate.edu

J.-M. Park, W. Leung
Ames Laboratory
US DOE, Iowa State University
Ames, IA 50011, USA

K. S. Nalwa, Prof. S. Chaudhary
Department of Electrical and Computer Engineering
Iowa State University
Ames, IA 50011, USA
E-mail: sumitc@iastate.edu

Prof. T.-G. Kim
School of Electrical Engineering
Korea University
Anam-dong, Seongbuk-Gu, Seoul 136–701, Korea

DOI: 10.1002/adma.201100419

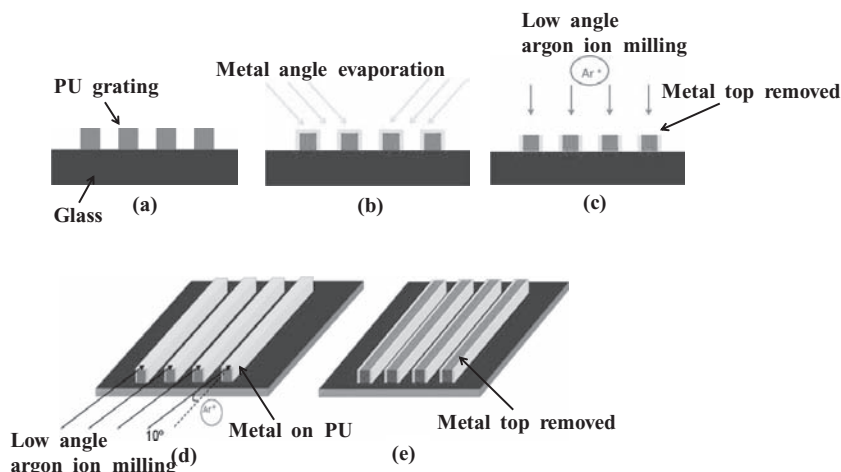


Figure 1. Schematics of the fabrication process. a) PU one-layer grating by 2-P μ TM on glass substrate, b) angle depositions of metal films on PU grating, and c) directional low-angle argon ion milling to remove the metal from the top. The argon ion milling step is shown separately in perspective views d) before and e) after the metal top surface is removed.

was uniformly patterned in one direction and the surface of the PU bars was smooth. The grating structure had a periodicity of 2.5 μ m, and the PU bar height and width were both \approx 1.2 μ m. The profile of the PU bars was isosceles-trapezoidal and had a base angle of \approx 80°. Typical samples had an area of 4 \times 4 mm², although larger samples have been made. As the SEM images (Figure 2c,d) show, the metal on top of the PU was completely stripped off, and the PU top surface was slightly etched with some roughness. Because the mechanical integrity of PU bars is not altered during the milling process, the metal layers on

the metallic structures leave most of the substrate area available for transmission of light, except for the nanoscale cross section that the thickness of the metallic sidewalls occupies. To characterize the light transmission behavior, we performed optical transmission measurements on the structures after the ion milling step. Due to the diffracting nature of the grating structure, an integrating sphere was used to collect the diffused light and to measure the total transmission through the sample. For comparison, the transmission of a standard commercially available ITO-coated glass was also measured. All the samples were measured with air as the reference. The ITO-coated glass had a peak transmission of 88% at around 600 nm and an average transmission of 82% over the entire optical wavelength range (400–800 nm). For a PU grating structure on glass without any metal, the total transmission spectrum was flat and was \approx 86%. The transmission of a PU thin film on glass was similar to glass at 92%. The reduced transmission of the PU grating was due to the additional diffractive reflection from the grating. For the ion milled patterned structures with metallic sidewalls, gold and silver showed similar transmission spectra. For gold, the peak total transmission was 84% at around 650 nm and the average total transmission was 80%. For silver, the peak transmission was 83% at around 650 nm and the average was \approx 78%. For two sidewalls of 40-nm-thick metal over the periodicity of 2.5 μ m, the reduction in transmission due to the metals is theoretically about 3%. Therefore, with the metallic sidewalls, the measured transmission dropped by an additional 6–8%. The additional reduction in transmission may be caused by some PU top-surface roughness, which results

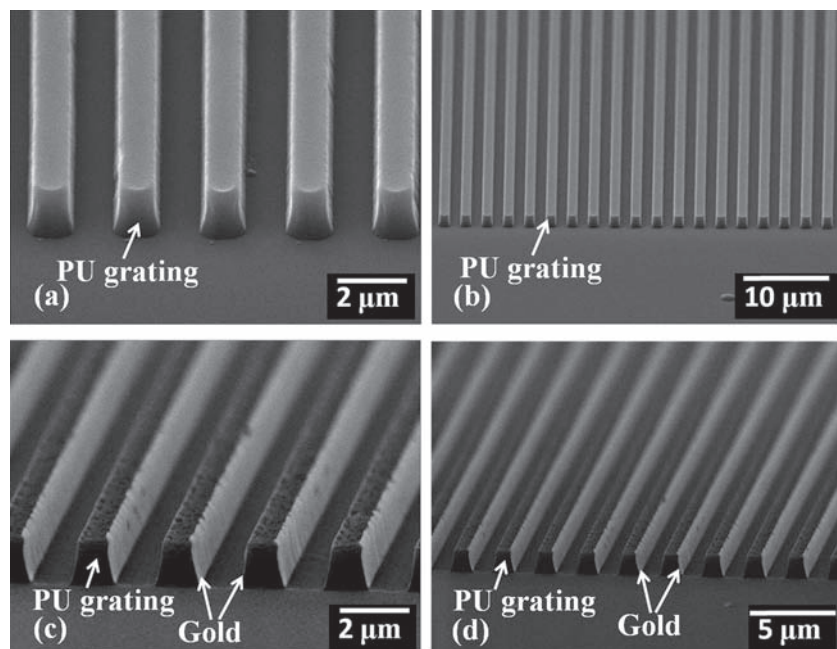


Figure 2. SEM images of a one-layer PU grating structure with 2.5- μ m periodicity by 2-P μ TM at a) high magnification and b) low magnification and of the argon ion milled sample with 40-nm gold sidewalls at c) high magnification and d) low magnification.

both PU sidewalls stay intact without defect or breakage. The height and thickness of the metal sidewalls were 1.2 μ m and 40 nm, respectively. This gives a very high (30:1) aspect ratio for the metallic films. Since metal was deposited on both sidewalls, the periodicity of the gold nanowire patterns was reduced by half to \approx 1.2–1.3 μ m. A structure with periods larger than optical wavelength is useful to improve optical properties (higher transmission and reduced diffraction), and the polarization effect does not take place in the visible wavelength range. Further details of the fabrication processes are given in the Experimental Section.

Two different metals, Au and Ag, were evaporated on separate one-layer PU grating samples by angle depositions, and the samples were subsequently argon ion milled to demonstrate that various metals can be deposited on the side walls using this fabrication method.

As the SEM images show (Figure 2c,d), the metallic structures leave most of the substrate area available for transmission of light, except for the nanoscale cross section that the thickness of the metallic sidewalls occupies. To characterize the light transmission behavior, we performed optical transmission measurements on the structures after the ion milling step. Due to the diffracting nature of the grating structure, an integrating sphere was used to collect the diffused light and to measure the total transmission through the sample. For comparison, the transmission of a standard commercially available ITO-coated glass was also measured. All the samples were measured with air as the reference. The ITO-coated glass had a peak transmission of 88% at around 600 nm and an average transmission of 82% over the entire optical wavelength range (400–800 nm). For a PU grating structure on glass without any metal, the total transmission spectrum was flat and was \approx 86%. The transmission of a PU thin film on glass was similar to glass at 92%. The reduced transmission of the PU grating was due to the additional diffractive reflection from the grating. For the ion milled patterned structures with metallic sidewalls, gold and silver showed similar transmission spectra. For gold, the peak total transmission was 84% at around 650 nm and the average total transmission was 80%. For silver, the peak transmission was 83% at around 650 nm and the average was \approx 78%. For two sidewalls of 40-nm-thick metal over the periodicity of 2.5 μ m, the reduction in transmission due to the metals is theoretically about 3%. Therefore, with the metallic sidewalls, the measured transmission dropped by an additional 6–8%. The additional reduction in transmission may be caused by some PU top-surface roughness, which results

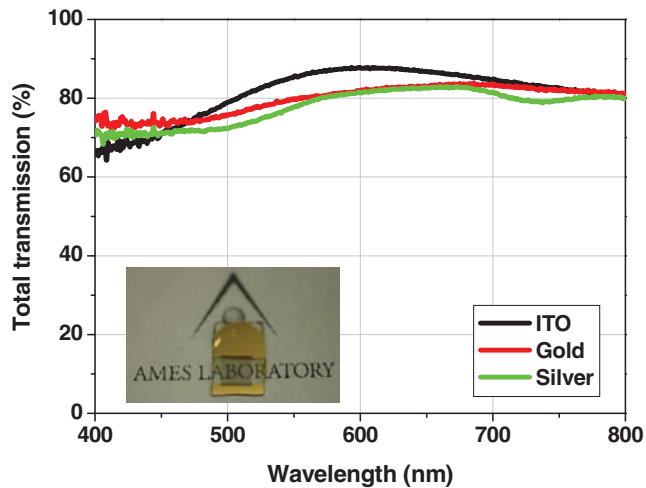


Figure 3. Total transmission of ITO-coated glass and 1-layer 2.5- μm -period PU grating structures on glass with 40-nm gold and silver sidewalls after argon ion milling.

in diffused scattering backwards. Nevertheless, the polarization effect was not severe since the periodicity of the samples was 2.5 μm , which shows great polarization contrast in the infrared wavelength regime. The inset in **Figure 3** shows an ion-milled sample with 40-nm gold sidewalls. The area of the sample was 4 \times 4 mm², and two metal contacts with 3-mm separation were deposited at two ends of the sample for electrical characterization.

To characterize the electrical conductivity, two-wire electrical measurements were performed to measure the resistance of the argon-ion-milled, high-aspect-ratio metallic structures. The resistance of the 2.5- μm structure with 40-nm gold sidewalls was measured to be 7.3 Ω . The resistance of the 2.5- μm structure with 40-nm silver sidewalls was measured to be 2.4 Ω . A typical ITO-coated glass has a sheet resistance around 10 $\Omega \square^{-1}$. For comparison, the resistance of a ITO-coated glass slab with a width of 4 mm (the same as our sample width) was measured with two parallel metal contacts deposited and also separated by about 3 mm on the slab. The measured resistance is about 7 Ω , which is close to that obtained by $R = R_{\text{sq}}L/W = 7.5 \Omega$, where R is the measured resistance of the sample, R_{sq} is the resistance per square, W is the width of the sample, and L is the distance of the two metal contacts deposited at two ends of the sample. Therefore, the resistance of the patterned gold structure after argon ion milling is equivalent to that of ITO-coated glass, and the resistance of patterned silver structure is three times less than that of ITO-coated glass. To calculate the sheet resistance of our structure, we used $R_{\text{sq}} = R(W/L)$. From the equation, we found the sheet resistance of patterned metallic structures with gold and silver were 9.7 $\Omega \square^{-1}$ and 3.2 $\Omega \square^{-1}$, respectively. Both values are less than the ITO sheet resistance typically used for organic LEDs and solar cells. Catrysse and Fan established a method for calculating the sheet resistance of nanopatterned metallic structures.^[12] Specifically for a 1D metallic grating structure, the sheet resistance can be calculated by $R_{\text{sq}} = (\rho/h)(a/w)$, where ρ is the bulk resistivity of metal, h is the height, a is the periodicity, and w is the width. The bulk resistivities

of gold and silver are $2.20 \times 10^{-8} \Omega \text{ m}$ and $1.59 \times 10^{-8} \Omega \text{ m}$, respectively.^[18] The calculated values of sheet resistance from the equation are 0.57 $\Omega \square^{-1}$ and 0.41 $\Omega \square^{-1}$ for gold and silver structure, respectively. The theoretical sheet resistances of our structures are more than tenfold lower than the measured ones. The first probable cause is that there is some breakage in the polymer template (disconnected PU bars) such that the metal sidewalls on such PU bars are not continuous and do not fully contribute to the electrical conduction. The second reason is the presence of nanograins formed during the metal thin-film deposition, which have significantly higher resistivities than the bulk.^[19] The grain boundary effect could be reduced by annealing the gold in ultrahigh vacuum and at high temperature to form larger and fewer grains.^[20,21] The much lower sheet resistance of the silver sample could be because silver does not experience as severe of a nanograin effect as gold.

To realize an organic or inorganic solar cell or LED on the transparent electrode platform, it is necessary to fill the open trenches with a transparent material to provide a flat area for the active layer deposition. We achieved this as shown in **Figure 4**.

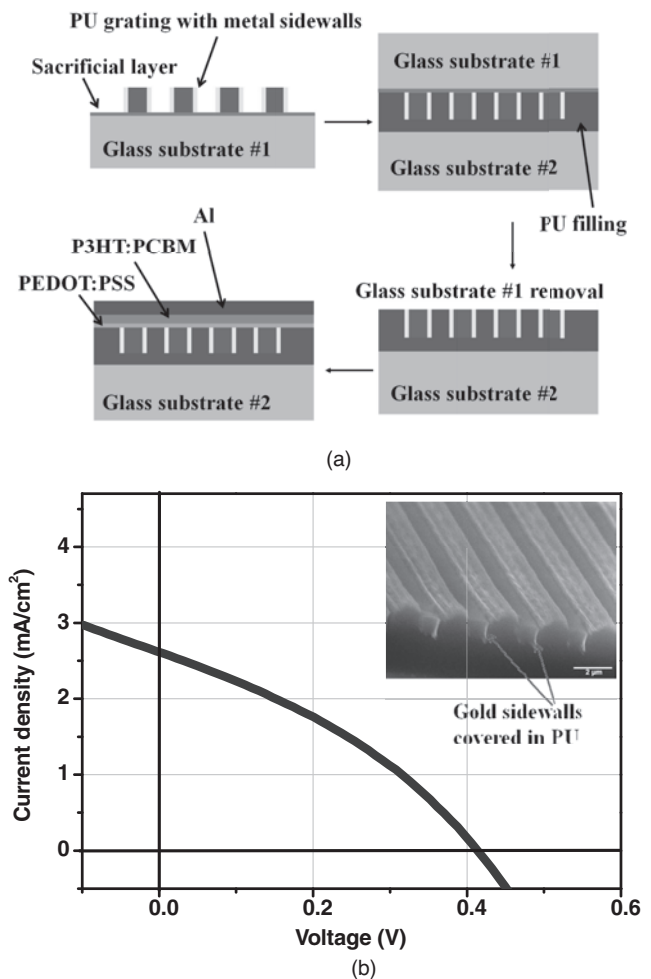


Figure 4. a) Schematics for sample inversion and organic active layer depositions and b) current density versus voltage characteristics of organic solar cells with the gold structure as the transparent electrode. The inset shows the inverted sample without active layers.

We first made the PU grating on a water-soluble sacrificial layer coated glass substrate. After metal deposition and argon ion milling, a small droplet of the PU prepolymer was placed on the sample to fill in the trenches of the grating structure. The PU prepolymer also served to glue a second glass substrate onto the sample. After the PU filling was ultraviolet cured and solidified, the sample was submerged in distilled water to dissolve the sacrificial layer and the original glass substrate was detached. Upon the separation of the original glass substrate, the bottom part of the structure was exposed and the sample was inverted. The inverted structure had an average total diffused transmission of $\approx 82\text{--}83\%$. This is because the filling of PU in the air gaps reduces diffraction from the grating structure; in addition, a smoother PU bottom surface is exposed. The resistance of the inverted structure was about $30\ \Omega$. The fact that the inverted sample had higher resistance than before inversion was probably due to overfilling of PU at the two ends of the sample, which would block the connections of the metal contacts to some of the metallic sidewalls during two-wire electrical measurements. As a proof-of-concept for applicability of the transparent electrodes, we fabricated a bulk heterojunction polythiophene:fullerene-based solar cell on the inverted structures. The current density versus voltage characteristics of the cell were then measured under illumination. The device successfully showed photovoltaic characteristics. However the performance was slightly inferior to typical ITO-electrode-based solar cells (usually short-circuit current is $\approx 8\text{--}10\ \text{mA cm}^{-2}$). Since the conductivity and transmittance of the transparent electrode was comparable to ITO, we believe that the performance of the solar cell is not similar to ITO-based devices because in some regions the top exposed regions of the gold sidewalls were partially covered by PU due to imperfect material processing prior to poly(3,4-ethylenedioxythiophene) doped with poly(styrenesulfonate) (PEDOT:PSS) deposition. SEM images in Figure 4b (inset) show evidence of such imperfections. Some contribution to poorer performance can also be ascribed to resistive losses due to horizontal transport of holes through the PEDOT:PSS layer, before they are collected by metal nanoribbons. However, this issue can be easily resolved by using highly conducting formulations of PEDOT:PSS, such as PH500. It has been shown that PH500 is able to efficiently transport holes over distances greater than 100 micrometers.^[22] The image shows that some metallic ribbons were embedded inside the polymer, and they were not exposed at the top. As a result, they may not have been in contact with PEDOT:PSS for charge transfer. However, this issue can be resolved by slightly etching the unnecessary polymer covering the metal electrode edges. In addition, the field enhancement at the interfacial contact between active layers and the electrodes may be a more vital issue than the optical improvement of the electrodes for achieving better performance efficiency of the device.

For applications such as solid-state lighting and smart windows, we have successfully made the structure with a larger sample area ($5 \times 5\ \text{cm}^2$), keeping the other dimensions the same. Additional PU prepolymer was used to fill the air channels between the metal sidewalls to reduce the diffraction effect from the grating pattern, and another glass substrate was bonded on top of the structure with the additional PU to form an encapsulated structure. It is likely that most applications

would require such encapsulation to protect the structure. It is demonstrated that, with the open trenches filled, the structure does not suffer a reduction in optical transmission even at very high incident angles ($>70^\circ$), and the diffraction is at an insignificant minimum. High transmission at steep incident angles is attributed to the higher refractive index of PU ($n \approx 1.5$), which replaces the low-index air gap as well as the PU overlayer. The application of additional PU for encapsulation effectively removes the original PU grating structure, which was the primary cause for the diffraction effect, resulting in thin vertically standing high-aspect-ratio metal bars with a periodicity of $\approx 1.2\text{--}1.3\ \mu\text{m}$. Furthermore, at the air/PU interface, if the incident angle of light is 60° , it is reduced to about 35° by refraction thereby guiding the light through the structure (see Supporting Information). The transmission of the encapsulated structures can be further improved by the adoption of various antireflection treatments at the encapsulation/air interface.

In summary, we have fabricated novel, patterned nanoscale metallic structures for use as transparent electrodes by a combination of two-polymer microtransfer molding, oblique metal deposition, and argon ion milling techniques. Such structures have high optical transparency, in the range of 80% for visible light, and low electrical resistance. Different metallic materials were deposited to show the feasibility of such a process to accommodate the requirements for various device applications. A working proof-of-principle organic solar cell device was fabricated. Furthermore, such transparent electrodes can be fabricated in large area and have important applications in smart windows and solid state lighting, and roll-to-roll processing can be realized for such structures in the foreseeable future.

Experimental Section

Thin Metallic Coating on the PU Gratings by Oblique Angle Depositions: After the PU gratings were made, a thin layer of metal ($\approx 40\text{nm}$), such as gold or silver, was deposited onto each PU bar by electron beam (e-beam) thermal evaporation. Since metal deposition at the normal incidence coated not only the PU bars but also the exposed substrate surface in between each PU bar, a stationary sample holder with a tilted angle (45°) was used so that the metal was only deposited on the sidewalls and the top of PU bars. This was important to maximize the optical transparency of the structure. The deposition rate for the metals was maintained at $0.1\ \text{nm s}^{-1}$ to ensure homogeneous metal coating. The e-beam evaporator pressure was maintained at 10^{-6} Torr during deposition. The metal thickness was chosen to be $\approx 40\ \text{nm}$ so that the sidewalls had narrow line widths to maximize the optical transmission of visible light.

Top Metallic Layer Removal Using the Argon Ion Milling Technique: To further improve the optical transparency of the structure, the metal layer on top of the PU bars was removed by argon ion milling (Gatan dual mill, model 600) at 3 kV and 1 mA at 2.8×10^{-4} Torr. First, the sample was positioned on the sample holder with the ion beam direction aligned parallel to that of the grating so that the metal sidewalls were not affected by the argon ions. The ion beam was also at a low incoming angle (10°) so the ion beam etched the metal top surface at a controllable rate and the ion beam covered a larger area. The milling time varied between 5 and 10 min depending on the materials and the top metal layer thickness. The PU top could be slightly etched by the argon ions as well.

Transparent Electrode Characterization and Organic Solar Cell Fabrication: The optical transmission of the samples was measured with a 3 inch labSphere integrating sphere with an Ocean Optics S2000

spectrometer. The electrical resistance was measured with a Fluke 8840A multimeter. For device fabrication, a conducting film of PEDOT:PSS (Clevios P VP Al 4083) was spin coated at 3000 rpm for 60 s on a standing Au grating substrate, followed by annealing at 60 °C for 5 min. The poly(3-hexylthiophene) and [6,6]-phenyl C61-butyrac acid methylester (P3HT:PCBM) blend solution (17 mg mL⁻¹ in dichlorobenzene) was spin-coated at 600 rpm for 30 s. An Al (200 nm) electrode (area = 3.14 mm²) was deposited by thermal evaporation on top of the active layer. Current density–voltage (*I*–*V*) measurements were done using a ELH Quartzline lamp with the intensity calibrated using a standard Si photodiode.

Supporting Information

Supporting Information is available from the Wiley Online Library or from the author.

Acknowledgements

The authors would like to thank Francis Laabs for assistance with the argon ion milling and Professor David Lynch for helpful discussions. This research is supported by the Division of Materials Sciences and Engineering, Basic Energy Sciences, US Department of Energy. The Ames Laboratory is operated by Iowa State University for the Office of Science, U.S. Department of Energy under Contract DE-AC02-07CH11358. Organic photovoltaic cell fabrication is also supported by the Iowa Power Fund from Iowa's Office of Energy Independence, plasma etching is supported by Korea Research Foundation grant funded by the Korean Government (MOEHRD) (KRF-2008-D00074) and a Korea Science and Engineering Foundation (KOSEF) grant funded by the Korea government (MOST) under project number [F01-2007-000-11760-0].

Received: February 2, 2011

Revised: February 22, 2011

Published online: April 29, 2011

- [1] Z. Chen, B. Cotterell, W. Wang, E. Guenther, S.-J. Chua, *Thin Solid Films* **2001**, 394, 202.
- [2] J. C. Scott, J. H. Kaufman, P. J. Brock, R. DiPietro, J. Salem, J. A. Goitia, *J. Appl. Phys.* **1996**, 79, 2745.
- [3] M. W. Rowell, M. A. Topinka, M. D. McGehee, H.-J. Prall, G. Dennler, N. S. Sariciftci, L. Hu, G. Gruner, *Appl. Phys. Lett.* **2006**, 88, 233506.
- [4] B. O'Connor, C. Haughn, K.-H. An, K. P. Pipe, M. Shtein, *Appl. Phys. Lett.* **2008**, 93, 223304.
- [5] J.-Y. Lee, S. T. Connor, Y. Cui, P. Peumans, *Nano Lett.* **2008**, 8, 689.
- [6] J.-Y. Lee, S. T. Connor, Y. Cui, P. Peumans, *Nano Lett.* **2010**, 10, 1276.
- [7] J. B. Wu, H. A. Becerril, Z. Bao, Z. Liu, Y. Chen, P. Peumans, *Appl. Phys. Lett.* **2008**, 92, 263302.
- [8] K. Tvingstedt, O. Inganäs, *Adv. Mater.* **2007**, 19, 2893.
- [9] M.-G. Kang, L. Guo, *Adv. Mater.* **2007**, 19, 1391.
- [10] M.-G. Kang, M.-S. Kim, J. Kim, L. Guo, *Adv. Mater.* **2008**, 20, 4408.
- [11] M.-G. Kang, H. J. Park, S.-H. Ahn, L. J. Guo, *J. Sol. Energy Mater. Sol. Cells* **2010**, 94, 1179.
- [12] P. B. Catrysse, S. Fan, *Nano Lett.* **2010**, 10, 2944.
- [13] J.-H. Lee, C.-H. Kim, K.-M. Ho, K. Constant, *Adv. Mater.* **2005**, 17, 2481.
- [14] K. R. Williams, K. Gupta, M. Wasilik, *J. Microelectromech. Sys.* **2003**, 12, 761.
- [15] X. D. Wang, E. Graugnard, J. S. King, Z. L. Wang, C. J. Summers, *Nano Lett.* **2004**, 4, 2223.
- [16] R. M. Ranade, S. S. Ang, W. D. Brown, *J. Electrochem. Soc.* **1993**, 140, 3676.
- [17] F. T. Aldridge, *J. Electrochem. Soc.* **1995**, 142, 1563.
- [18] D. R. Lide, *CRC Handbook of Chemistry and Physics*, 90th edition, CRC Press, Boca Raton, FL **2009**.
- [19] J. M. Camacho, A. I. Oliva, *Thin Solid Films* **2006**, 515, 1881.
- [20] C. V. Thompson, *Annu. Rev. Mater. Sci.* **1990**, 20, 245.
- [21] J. M. Park, K. S. Nalwa, W. Leung, K. Constant, S. Chaudhary, K. M. Ho, *Nanotechnology* **2010**, 21, 215301.
- [22] M. R. Lee, R. D. Eckert, K. Forberich, G. Dennler, C. J. Brabec, R. A. Gaudiana, *Science* **2009**, 324, 232.